GSA Data Repository 2018380

Mulder, J.A., et al., 2018, Rodinian devil in disguise: Correlation of 1.25–1.10 Ga strata between Tasmania and Grand Canyon: Geology, https://doi.org/10.1130/G45225.1.

Table DR1: Zircon U-Pb isotope data and methods

Table DR2: Zircon Hf isotope data and methods

Item DR3

Correlation chart of simplified stratigraphy

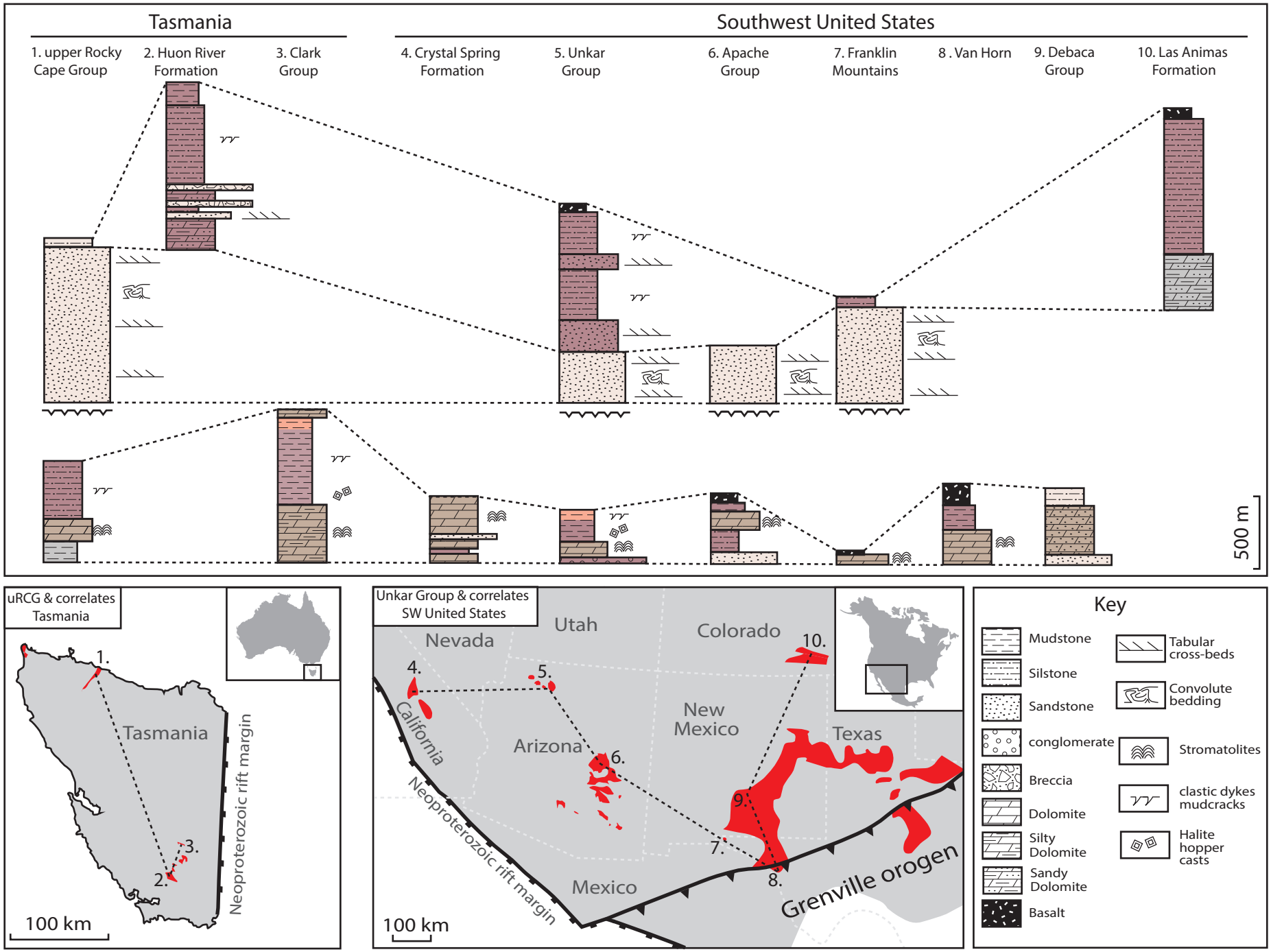

upper Rocky Cape Group, northwest Tasmania

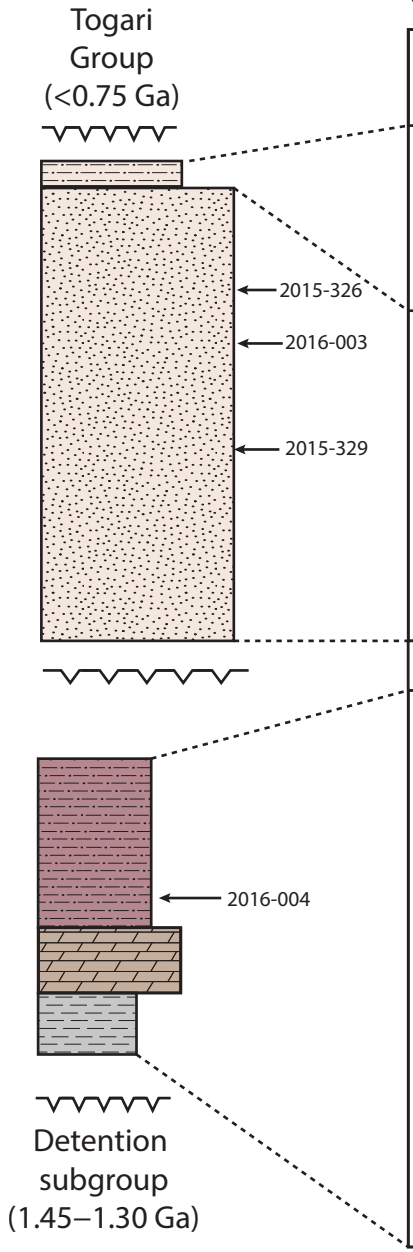

Name	Age Constraints	Thickness	Lithologies	Sedimentary Structures	Depositional Environments	References
Silstone Unit (unamed)	Conformable with underlying Jacob Quartzite	60 m (minimum)	Thinly interbedded, light brown to tan micaceous quartz silstone, and quartz sandstone	Planar lamination	Shallow marine	Gee (1967)
Jacob Quartzite	Max: 1170 ± 16 Ma (Youngest detrital zircon population) Min: <750 Ma from overlying Togari Group	1100 m	<1 m tabular beds of medium–coarse quartz arenite. tabular cross-bedding common throughout. <0.5 m-thic beds of micaceous silstone in upper parts	Tabular cross-beds, convolute folding, ripple marks	Shallow marine, high-energy, nearshore	Gee (1967)
Disconformity inferred from abrupt change in depositional setting and shift in detrital zircon provenance						
Irby Siltstone	Max: 1258 ± 16 Ma (Youngest detrital zircon population) Min: <750 Ma from overlying Togari Group	680 m	Black mudstone, maroon-grey-green silstone, quartz sandstone, dolomitic mudstone, dolomitic, silstone, dolostone, stromatolitic dolomite	Slump folds sandstones: planar lamination, cross-bedding, climbing ripple lamination, ripple marks. Silstone: clastic dykes, polygonal cracks Dolomite: microbial lamination, stromatolites, ooids, peloids, molar tooth structure	Shallow marine, periodically subaerial, low energy possibly, a sub- tidal to supra-tidal mudflat	Gee (1967) Calver & Baillie (1990) Seymour (2002)

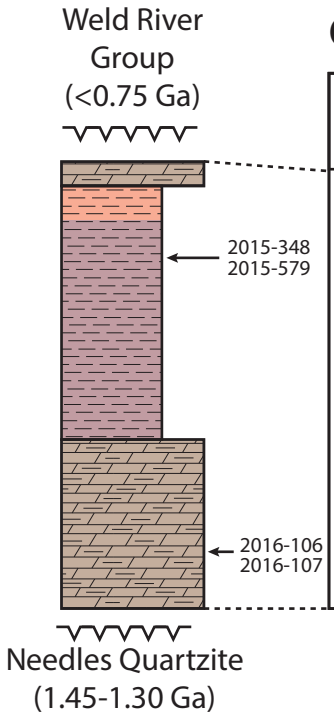

Clark Group, southern Tasmania

Name	Age Constraints	Thickness	Lithologies	Sedimentary Structures	Depositional Environments	References
Humboldt Formation	Max: 1329 ± 20 Ma (Youngest detrital zircon population) Min: <750 Ma from overlying Weld River Group	(?)2000 m (disrupted by faulting)	Dolomitic mudstone, dolostone, stromatolitic dolomite, shale, red and orange mudstone, red siltstone, chert, flat-pebble conglomerate, quartz arenite	Clastic dykes, halite hopper casts, molar tooth structure, (?)anhydrite nodules, oolites, stromatolites	Shallow marine, periodically subaerial, low energy possibly a sub- tidal to supra-tidal mudflat	Calver et al. (2006)

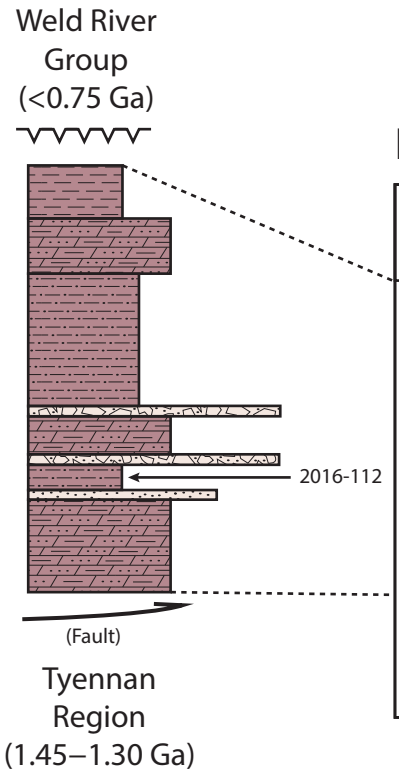

Huon River Formation, southern Tasmania

Name	Age Constraints	Thickness	Lithologies	Sedimentary Structures	Depositional Environments	References
Huon River Formation	Max: 1179 ± 13 Ma (Youngest detrital zircon population) Min: <750 Ma from overlying Weld River Group	(?)3000 m (disrupted by faulting)	red-purple-green mudstone and silstone, quartz arenite, intra-clastic breccia, dolostone	Clastic dykes, cross-bedding, ripple marks, chert nodules.	Shallow marine, periodically subaerial, mostly low energy, possibly a sub- to supra-tidal mudflat. Abundant breccia beds in lower parts suggest syn-depositional tectonism	Calver (1990)

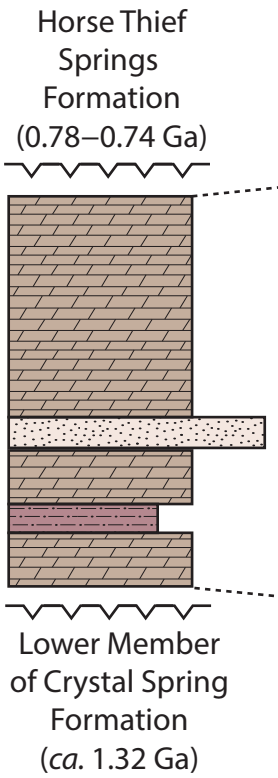

Crystal Spring Formation (Pahrump Group), Death Valley, California, USA

Name	Age Constraints	Thickness	Lithologies	Sedimentary Structures	Depositional Environments	References
Middle Member	Max: *ca.* 1210 Ma (Youngest detrital zircon population) Min: 1069 ± 3 Ma (cross-cutting diabse)	135–400 m	Dolomitic limestone, stromatolitic dolomite, quartz sandstone, silstone, mudstone	Stromatolites	Shallow marine	Roberts (1982) Heaman & Grotzinger (1992) Mahon et al. (2014) Mulder et al. (2017)

Unkar Group, Grand Canyon, Arizona, USA

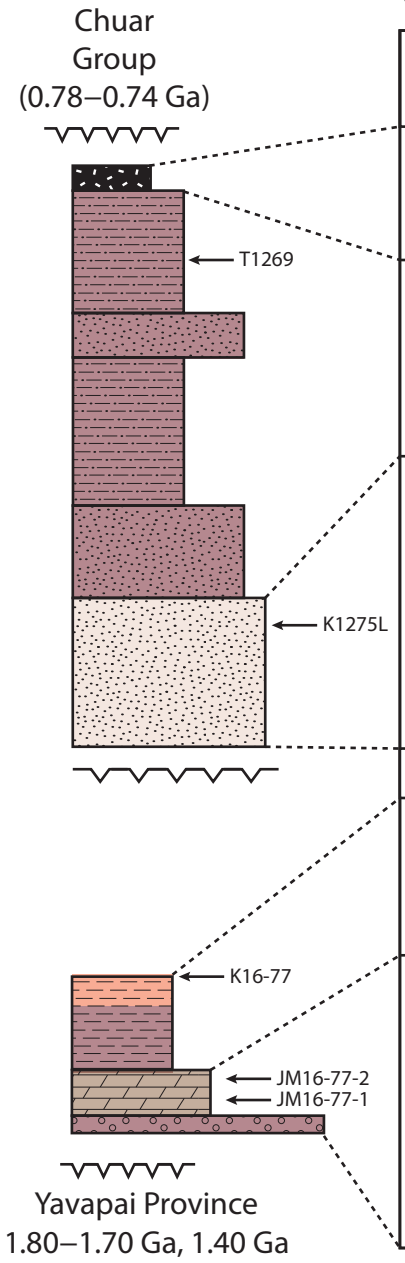

Name	Age Constraints	Thickness	Lithologies	Sedimentary Structures	Depositional Environments	References
Cardenas Basalt	1104 Ma	300 m	Basaltic lava flows and asscoiated volcani-clastic rocks		Intracratonic rift	Hendricks (1972) Larson et al. (1994) Weil et al. (2003) Timmons et al. (2005)
Dox Formation	Upper parts interlayered with 1104 Ma Cardenas Basalt	1000–1500 m	Red and maroon quartz sandstone, arkose, micaceous sandstone, and mudstone	Tabular cross-bedding, partling lineations, trouchs, clastic dykes, ripples marks	Deltaic and shallow marine	Stevenson and Beus (1982) Timmons et al. (2005) Mulder et al. (2017)
Shinumo Sandstone	Max: 1184 ± 5 Ma (Youngest detrital zircon population)	200–300 m	<2 m thick beds of medium-coarse quartz arenite, minor silstone and mudstone Tabular cross-bedding common throughout	Tabular cross-bedding, ripple marks, convolute folding	High energy shallow marine, supra-tidal mudflat, fluvial, deltaic	Daneker (1975) Middleton and Blakey (1998) Timmons et al. (2005) Mulder et al. (2017)
Disconformity inferred from abrupt change in depositional setting and shift in detrital zircon provenance						
Hakatai Shale	Max: 1243 ± 2 Ma (Youngest detrital zircon population)	100–300 m	Red and orange mudstone, arkose	Clastic dykes, polygonal cracks, ripple marks, halite hopper casts	Sub- to supra-tidal mudflats, shallow marine	Reed (1976) Timmons et al. (2005) Bloch et al. (2006) Mulder et al. (2017)
Bass Formation	Lower parts interlayered with a felsic tuff dated at 1254.8 ± 1.6 Ma	60–100 m	Stromatolitic dolomite, quartz sandstone, arkose, silstone, mudstone, felsic tuff, conglomer-ates in lower parts and at base	Tabular cross-bedding, ripple marks, clastic dykes, polygonal cracks, microbial lamination, stromatolites	Low energy shallow marine, sub- to supra-tidal mudflats, conglomerates record syn-depositional seismicity	Dalton (1972) Timmons et al. (2005) Mulder et al. (2017)

Apache Group, eastern Arizona, USA

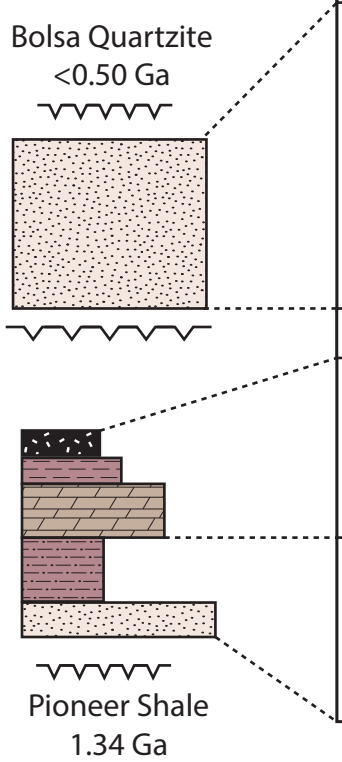

Name	Age Constraints	Thickness	Lithologies	Sedimentary Structures	Depositional Environments	References
Troy Quartzite	Max: 1259 ± 1.7 Ma (Youngest detrital zircon population) Min: 1080 Ma (cross-cutting dolerite dyke)	365 m (minimum)	Tabular bedded arkose, quartz-arenite, silstsone, mudstone, conglomerate	Cross-bedding (tabular and trough), ripplemarks, convolute folding	Fluvial floodplain and braided stream complex, eolian, high energy shallow marine	Schride (1967) Weiss (1986) Burns (1987) Wrucke (1989) Mulder et al. (2017)
Unconformity inferred from, minor folding of Mescal Limestone, abrupt change in depositional setting						
Mescal Limestone	Min: 1080 Ma (cross-cutting dolerite dyke)	75–130 m	Laminated dolomite, stromatolitic dolomite, chert, conglomerate, mudstone, silstone, basaltic lava	Stromatolites, slump folds	Low energy shallow marine	Schride (1967) McConnel (1975) Bertrand-Sarfati and Awramik (1992)
Dripping Springs Formation	Max: 1256 ± 3 Ma (Youngest detrital zircon population)	170–215 m	Arkose, siltstone, mudstone	Tabular cross-bedding, scour and fill structures	sub- to supra-tidal mud flats, distal alluvial fans	Shride (1967) Engel and Elmore (1990) Middleton and Montgomery (2001) Beraldi-Campesi et al. (2014)

Debaca Group, Texas and New Mexico, USA

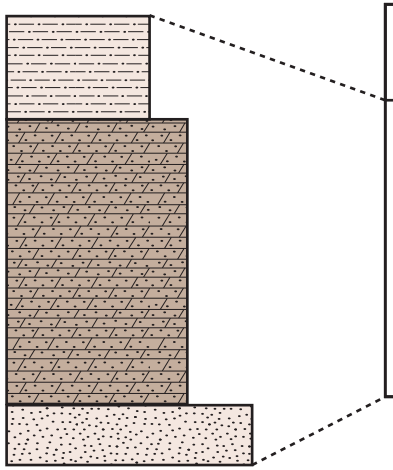

Name	Age Constraints	Thickness	Lithologies	Sedimentary Structures	Depositional Environments	References
Debaca Group	Max: 1334 ± 52 Ma (underlying basement) Min: 1090 ± 4 Ma (cross-cutting gabbro intrusive)	500 m (approximate)	Arkose, quartzite, micaceous silstone, shale, quartz-rich dolomite, dolomitic quartzite, felsic volcaniclastic silt-stone and sandstone, rhyolite	Tabular cross-bedding, clastic dykes, polygonal cracks	Shallow marine	Pary (1961) Amarante (2001)

Franklin Mountains, western Texas, USA

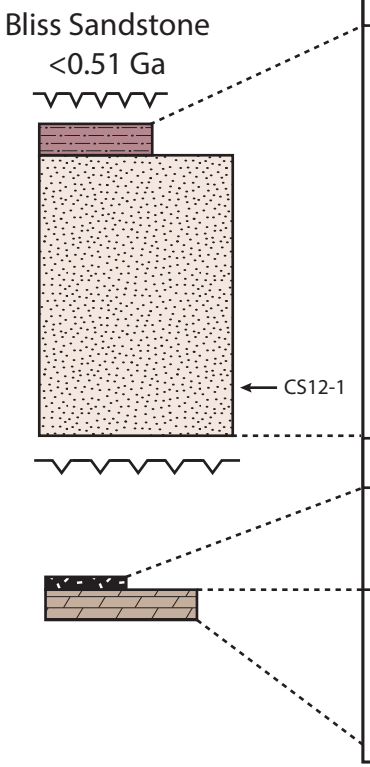

Name	Age Constraints	Thickness	Lithologies	Sedimentary Structures	Depositional Environments	References
Llanoria Formation	Max: 1229 ± 3 Ma (Youngest detrital zircon population from Mulder et al. 2017) Max: 1130 Ma (Youngest detrital zircon population from Spencer et al. 2014) Min: 1120 ± 35 Ma (cross-cutting Red Bluff Granite)	739 m	Tabular bedded quartz arenite, sub arkose, and mudstone red-maroon sandstone and silstone in upper parts	Tabular cross-bedding, ripple marks, convulte folding	High-energy, tidally dominated shallow marine shelf. Upper parts deltaic	Seeley (1999) Spencer et al. (2014) Mulder et al. (2017)
Disconformity inferred from abrupt change in depositional setting						
Mundy Breccia	Synchronous with Castner Marble	70 m	Basaltic breccia, massive basalt, agglomerate	Megablocks of Castner Marble	subaqueous gravity flows	Pittenger et al. (1994)
Castner Marble	Interbedded with felsic tuffs dated at 1251 ± 47 Ma, 1260 ± 20 Ma, 1272 ± 5 Ma	100 m (minimum)	Limestone, rhythmite, flat-pebble conglomerate, tuffaceous silstone, felsic tuffs	Stromatolites	Sub-tidal to supra -tidal carbonate ramp	Pittenger et al. (1994)

Van Horn, western Texas, USA

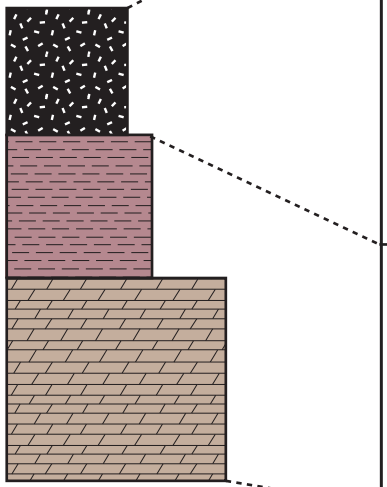

Name	Age Constraints	Thickness	Lithologies	Sedimentary Structures	Depositional Environments	References
Tumbledown Formation	Max: 1243 ± 10 Ma (rhyolite clast in basal lithic arenite) Min: <510 Ma disconformably overlying Bliss Sandstone	168 m	Volcanic lithic arenite, pillow basalt, basaltic breccia, agglomerate, and flows		Intracontinental rift	Soegaard and Callahan (1994) Bickford et al. (2000) Spencer et al.(2014)
Allamoore Formation	Interbedded with felsic tuffs dated at 1253 ± 15 Ma, 1256 ± 5 Ma, 1250 + 20/ -27 Ma	324 m	Interbedded dolostone and chert, talc rock, mudstone, felsic tuff, pillow basalt, basalt flows and hyaloclastic breccia	Stromatolites, halite hopper casts	Sub- to supra-tidal mudflats	King & Flawn (1953) Edwards (1984) Soegaard and Callahan (1994) Roths (1993) Bickford et al. (2000)

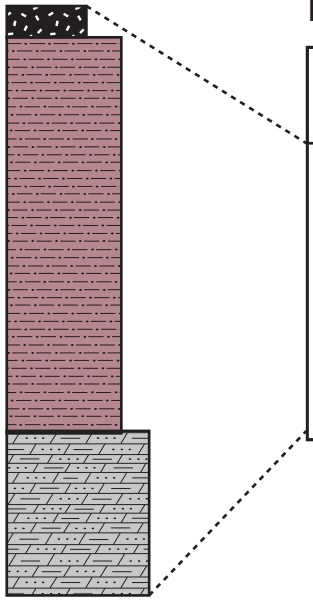

Las Animas Formation, Colorado, USA

Name	Age Constraints	Thickness	Lithologies	Sedimentary Structures	Depositional Environments	References
Las Animas Formation	Max: *ca.* 1400 Ma (underlying basement)	1700 m	Greywacke, mudstone, chert, red-maroon arkose, dolomite, conglomerate, andesitic and basaltic lava and tuffs		Shallow marine	Tweto (1983)

References Cited

Amarante, J.F.A., 2001. Characteristic of the basement rocks in the Mescalero 1 well, Guadalupe County, New Mexico (M.S. thesis). New Mexico Institute of Mining and Technology, Socorro, p. 73.

Beraldi-Campesi, H., Farmer, J.D., Garcia-Pichel, F., 2014. Modern terrestrial sedimentary biostructures and their fossil analogs in mesoproterozoic subaerial deposits. Palaios 29, 45–54.

Bertrand-Sarfati, J., Awramik, S.M., 1992. Stromatolites of the mescal limestone (Apache Group, Middle Proterozoic, Central Arizona) – taxonomy, biostratigraphy, and paleoenvironments. Geol. Soc. Am. Bull. 104, 1138–1155.

Bickford, M.E., Soegaard, K., Nielsen, K.C., McLelland, J.M., 2000. Geology and geochronology of Grenville- age rocks in the Van Horn and Franklin Mountains area, west Texas; implications for the tectonic evolution of Laurentia during the Grenville. Geol. Soc. Am. Bull. 112, 1134–1148.

Bloch, J., Timmons, M., Crossey, L.J., Gehrels, G.E., Karlstrom, K.E., 2006. Mudstone petrology of the Mesoproterozoic Unkar Group, Grand Canyon, U.S.A.: Provenance, weathering, and sediment transport on intracratonic Rodinia. J. Sediment. Res. 76, 1106–1119.

Burns, B.A., 1987. The Sedimentology and Significance of a Middle Proterozoic braidplain; Chediski Sandstone Member of the Troy Quartzite, central Arizona (M.S. thesis). Northern Arizona University, Flagstaff, p. 143.

Calver C. R.. 1990. Huon River Formation. In: Calver, C.R. , Turner, N.J. , McClenaghan, M.P. , McClenaghan, J. Pedder,Tasmania. 1:50,000 Sheet 80(8112S). Geological Survey of Tasmania.

Calver, C. R., and Baillie, P. W., 1990. Early diagenetic concretions associated with intrastratal shrinkage cracks in an upper Proterozoic dolomite, Tasmania, Australia. Journal of Sedimentary Petrology, v. 60, 293—305.

Calver, C. R., Forsyth, S. M., Everard, J. L., 2006. Geology of the Skeleton, Nevada, Weld and Picton 1:25 000 scale map sheets. Tasmanian Geological Survey Record 2006/4.

Dalton Jr., R.O., 1972. Stratigraphy of the Bass Formation (Late Precambrian, Grand Canyon, Arizona) (M.S. thesis). Northern Arizona University, Flagstaff, p. 140.

Daneker, T.M., 1975. Sedimentology of the Precambrian Shinumo Sandstone, Grand Canyon, Arizona (M.S. thesis). Northern Arizona University, Flagstaff, p. 195.

Engel, M.H., Elmore, R.D., 1990. Assessments of the Hydrocarbon Generation Potential of Selected North American Proterozoic Rock Sequences. Progress Report for the U.S. Department of Energy.

Gee, R.D., 1967. The tectonic evolution of the Rocky Cape Geanticline. PhD Thesis [unpub.], University of Tasmania.

Heaman, L.M., Grotzinger, J.P., 1992. 1.08 Ga diabase sills in the Pahrump Group, California: Implications for development of the Cordilleran miogeocline. Geology 20, 637–640.

Hendricks, J.D., 1972. Younger Precambrian Basaltic Rocks of the Grand Canyon, Arizona (M.S. thesis). Northern Arizona University, Flagstaff, p. 122.

Larson, E.E., Patterson, P.E., Mutschler, F.E., 1994. Lithology, chemistry, age, and origin of the Proterozoic Cardenas Basalt, Grand Canyon, Arizona. Precambr. Res. 65 (1–4), 255–276.

Mahon, R.C., Dehler, C.M., Link, P.K., Karlstrom, K.E., Gehrels, G.E., 2014. Detrital zircon provenance and paleogeography of the Pahrump Group and overlying strata, Death Valley, California. Precambr. Res. 251, 102–117.

McConnell, R.L., 1975. Biostratigraphy and depositional environment of algal stromatolites from the Mescal Limestone (Proterozoic) of central Arizona. Precambr. Res. 2, 317–328.

Middleton, L.T., Blakey, R.C., 1998. Seismically induced liquefaction in late Proterozoic strata, northern and central Arizona; implications for tectonic setting and regional correlations: Geological Society of America Abstracts with Programs, 30(2), p. 399.

Middleton, L.T., Montgomery, M.W., 2001. Sedimentary responses to changing tectonic patterns, Mesoproterozoic Apache Group/Troy Quartzite, Central Arizona, in Rocky Mountain (53rd) and South-Central (35th) Sections, Geological Society of America, Joint Annual Meeting; April 29–May 2, 2001; Albuquerque, New Mexico, Session No. 11.

Pittenger, M.A., Marsaglia, K.M., Bickford, M.E., 1994. Depositional history of the Middle Proterozoic Castner Marble and basal Mundy Breccia, Franklin Mountains, west Texas. J. Sediment. Res. B64, 282–297.

Pray, L.C., 1961. Geology of the Sacramento Mountains Escarpment, Otero County, New Mexico: New Mexico Bureau of Mines and Mineral Resources, Bulletin 35, 144 p.

Reed, V.S., 1976. Stratigraphy and Depositional Environment of the upper Precambrian Hakatai Shale, Grand Canyon, Arizona (M.S. thesis). Northern Arizona University, Flagstaff, p. 163.

Roberts, M.T., 1982. Depositional environments and tectonic setting of the Crystal Spring Formation, Death Valley, California. In: Cooper, J.D., Troxel, B.W., Wright, L.A. (Eds.), Geology of Selected Areas in the San Bernardino Mountains, Western Mojave Desert, and Southern Great Basin, California: Volume and Guidebook for Field Trip no. 9, 78th Anniversary Meeting of Cordilleran Section. Geological Society of America. Death Valley Publishing Company, Shoshone, CA, pp. 165– 170.

Roths, P.J., 1993. Geochemical and geochronological studies of the Grenville-age (1,250–1,000 Ma) Allamoore and Hazel Formations, Hudspeth and Culberson counties, west Texas. In: Soegaard, K. et al. (Eds.), Precambrian Geology of the Franklin Mountains and Van Horn Area, Trans-Pecos Texas. Geological Society of America South Central Section, University of Texas, Dallas, Texas, pp. 11–35.

Seeley, J., 1999. Studies of the Proterozoic Tectonic Evolution of the Southwestern United States (Ph.D. thesis). University of Texas, El Paso, p. 321.

Seymour, D. B. compiler 2002. Marrawah West, Tasmania. Digital Geological Atlas 1:25000 Series Map Sheet. Mineral Resources Tasmania.
Shride, A.F., 1967. Younger Precambrian geology in southern Arizona. U.S. Geol. Surv. Prof. Pap. 566, 88.

Soegaard, K., Callahan, D.M., 1994. Late Middle Protero- zoic Hazel Formation near Van Horn, trans-Pecos Texas: evidence for transpressive deformation in Grenvillian basement. Geol. Soc. Am. Bull. 106, 413–423.

Spencer, C.J., Prave, A.R., Cawood, P.A., Roberts, N.M.W., 2014. Detrital zircon geochronology of the Grenville/Llano foreland and basal Sauk Sequence in west Texas, USA. Geol. Soc. Am. Bull. 126, 1117–1128.

Stevenson, G.M., Beus, S.S., 1982. Stratigraphy and depositional setting of the upper precambrian dox formation in grand-canyon. Geol. Soc. Am. Bull. 93, 163–173.

Timmons, J.M., Karlstrom, K.E., Heizler, M.T., Bowring, S.A., Gehrels, G.E., Crossey, L. J., 2005. Tectonic inferences from the ca. 1255–1100 Ma Unkar Group and Nankoweap Formation, Grand Canyon: intracratonic deformation and basin formation during protracted Grenville orogenesis. Geol. Soc. Am. Bull. 117, 1573–1595.

Tweto, O., 1983. Las Animas Formation (Upper Precambrian) in the Subsurface of Southeastern Colorado U.S. Geological Survey Bulletin 1529-G, p. 20.

Weil, A.B., Geissman, J.W., Heizler, M., Van der Voo, R., 2003. Paleomagnetism of Middle Proterozoic mafic intrusions and Upper Proterozoic (Nankoweap) red beds from the Lower Grand Canyon Supergroup, Arizona. Tectonophysics 375, 199–220.

Weiss, G.C., 1986. A depositional Analysis of the Arkose Member (middle Proterozoic) of the Troy Quartzite in Central Arizona (M.S. thesis). Northern Arizona University, Flagstaff, p. 382.

Wrucke, C.T., 1989. The middle Proterozoic Apache Group, Troy Quartzite, and associated diabase of Arizona: Arizona Geological Society Digest, 17, pp. 239– 258.

DR4: Palaeomagnetic data

Three GPlates files are supplied with this submission. In order to visualise the reconstruction, users need to download and install GPlates from www.gplates.org, instructions on how to use GPlates are found at that website.

List and description of files:

1) Mulder_2018_polygons.gpml

Contains the polygons for the key components used in this reconstruction: Australia, Laurentia, Antarctica, Tasmania, East and West South Tasman Rise, Coats Land Block, Kalahari.

2) Mulder_2018_rotations.rot

Contains the Euler Pole rotations that describe the relative and absolute motions of the polygons used in the reconstruction. Rotation file is only valid from 1140 to 900 Ma. References to published Euler Poles are included in the rotation file.

3) Mulder_2018_palaeomagnetic_data.gpml

Contains all the palaeomagnetic data listed in DM 4. To visualise data, users must:

i) Load it into GPlates
ii) Open the 'Layers Pallete' (Control/Alt +L)
iii) Expand the layer labeled 'Mulder_2018_palaeomagnetic_data'
iv) Click on 'Set VGP visibility...'
v) Click on 'Show all VGPs at all times'

Palaeomagnetic data should then be visible for the age specific time.

Table D4: List of palaeomagnetic data from Australia and Laurentia around 1.4 Ga used to constrain reconstruction in Figure 3. sLat and Slon refer to the site latitude and longitude of the pole, pLat and pLon refer to the pole latitude and longitude. See supplementary material 5 for *GPlates* reconstruction files.

Code	Name	Young Age (Ma)	Old Age (Ma)	sLat (°N)	sLon (°E)	pLat (°N)	pLon (°E)	a95 (°)	Reference
AUS1	Mt. Isa dolerite dykes	1139	1141	-20.5	139.5	9.5	311.1	17.4	Tanaka and Idnurm, 1994
AUS2	Bangemall Sills	1064	1076	-23.5	116.5	33.9	95	8.3	Wingate et al. 2002
LAU1	Abitibi Dyles	1139	1143	48	-81	44.4	211.4	13.7	Ernst and Buchan, 1993
GRL1	Giant gabbro dykes	1161	1165	61.2	311.7	42.3	226.1	9.4	Piper, 1977; Buchan et al. 2001
GRL2	South Qoroq intrusions	1161	1165	61.2	-45.4	41.8	215.9	13.1	Piper, 1992
GRL3	NE-trending dyke swarm	1155	1165	61.2	-45.4	33.4	230.8	5.7	Piper, 1992
LAU2	Osler Group (Upper Reversed)	1103	1107	48.9	-87.7	42.5	201.6	3.7	Swanson-Hysell et al., 2014a
LAU3	Mamainse Point (lower normal, upper reversed)	1099	1101	47	-84.8	36.1	189.7	4.9	Swanson-Hysell et al., 2014b
LAU4	North Shore Volcanic Group (Upper SW sequence)	1095	1100	47	-91.8	35.8	182.1	3.1	Tauxe and Kodama (2009)
LAU5	Portage Lake Volcanics	1090	1100	47.5	-88.5	27.1	182	2.2	Books 1972; Hnat et al., 2006
LAU6	Schroeder-Lutsen basalts (no lower age constraint)	1080	1091	47.5	-91	27.1	187.8	3	Fairchild et al. 2017; Tauxe and Kodama (2009)
LAU7	Lake Shore traps	1083	1087	47.5	-88	23.1	186.4	4	Fairchild et al. 2017
LAU8	Michipicoten Island Formation	1083	1085	47.5	-86	17	174.7	4.4	Fairchild et al. 2017
LAU9	Nonesuch Shale (	1075	1085	46.5	-89.3	7.3	174.7	3	Symons et al. (2013); Henry et al. (1977)
LAU10	Freda Sandstone (no upper age constraint)	1070	1080	46.5	-88	2.2	179	5.9	Henry et al. 1977
LAU11	Jacobsville Sanstone (no lower age constraint)	1060	1065	46.5	-88	-10	184	4.3	Roy and Robertson (1978)
CLB1	Coats Land Nunataks	1103	1109	-78	-35	23	80	7	Gose et al., 1997
KAL1	Umkondo Ingeous Province	1107	1113	-25	29	-66	-143	3	Gose et al., 2006
KAL2	Central Namaqua Belt	1030	1000	-30	20	-8	150	10	Onstott et al., 1986, *cited in Jacobs et al., 2008*
KAL3	Port Edward Pluton	1009	999	-31	30	7	148	4	Gose et al., 2004
LAU12	Haliburton Intrusions	1030	1000	45	-77	-36	143	6	Warnock et al., 2000

References:

Books, K.G., 1972. Paleomagnetism of some Lake Superior Keweenawan rocks. In *Geological Survey professional paper* (v. 760). US Government Printing Office.

Buchan, K.L., Ernst, R.E., Hamilton, M.A., Mertanen, S., Pesonen, L.J. and Elming, S.Å., 2001. Rodinia: the evidence from integrated palaeomagnetism and U–Pb geochronology. *Precambrian Research*, *110*(1-4), pp.9-32, doi: 10.1016/S0301-9268(01)00178-4

Ernst, R.E. and Buchan, K.L., 1993. Paleomagnetism of the Abitibi dyke swarm, southern Superior Province, and implications for the Logan Loop. *Canadian Journal of Earth Sciences*, *30*(9), pp.1886-1897, doi: 10.1139/e93-167

Fairchild, L.M., Swanson-Hysell, N.L., Ramezani, J., Sprain, C.J. and Bowring, S.A., 2017. The end of Midcontinent Rift magmatism and the paleogeography of Laurentia. *Lithosphere*, *9*(1), pp.117-133.

Gose, W.A., Helper, M.A., Connelly, J.N., Hutson, F.E. and Dalziel, I.W., 1997. Paleomagnetic data and U□Pb isotopic age determinations from Coats Land, Antarctica: Implications for late Proterozoic plate reconstructions. *Journal of Geophysical Research: Solid Earth*, *102*(B4), pp.7887-7902.

Gose, W.A., Johnston, S.T. and Thomas, R.J., 2004. Age of magnetization of Mesoproterozoic rocks from the Natal sector of the Namaqua-Natal belt, South Africa. *Journal of African Earth Sciences*, *40*(3-4), pp.137-145.

Gose, W.A., Hanson, R.E., Dalziel, I.W., Pancake, J.A. and Seidel, E.K., 2006. Paleomagnetism of the 1.1 Ga Umkondo large igneous province in southern Africa. *Journal of Geophysical Research: Solid Earth*, *111*(B9).

Henry, S.G., Mauk, F.J. and der Voo, R.V., 1977. Paleomagnetism of the upper Keweenawan sediments: the Nonesuch Shale and Freda Sandstone. *Canadian Journal of Earth Sciences*, *14*(5), pp.1128-1138.

Hnat, J.S., Van der Pluijm, B.A. and Van der Voo, R., 2006. Primary curvature in the Mid-Continent Rift: Paleomagnetism of the Portage Lake Volcanics (northern Michigan, USA). *Tectonophysics*, *425*(1-4), pp.71-82.

Jacobs, J., Pisarevsky, S., Thomas, R.J. and Becker, T., 2008. The Kalahari Craton during the assembly and dispersal of Rodinia. *Precambrian Research*, *160*(1-2), pp.142-158.

Onstott, T.C., Hargraves, R.B., Joubert, P., 1986. Constraints on the tectonic evolution of the Namaqua Province II: reconnaissance palaeomagnetic and 40Ar/39Ar results from the Namaqua Province and the Kheis Belt. *Transactions of the Geological Society of South Africa,* 89, 143–170.

Piper, J.D.A., 1992. The palaeomagnetism of major (Middle Proterozoic) igneous complexes, South Greenland and the Gardar apparent polar wander track. *Precambrian Research*, *54*(2-4), pp.153-172, doi: 10.1016/0301-9268(92)90068-Y

Piper, J.D.A. and Stearn, J.E.F., 1977. Palaeomagnetism of the dyke swarms of the Gardar Igneous Province, South Greenland. *Physics of the Earth and Planetary Interiors*, *14*(4), pp.345-358, doi: 10.1016/0031-9201(77)90167-4

Roy, J.L. and Robertson, W.A., 1978. Paleomagnetism of the Jacobsville Formation and the apparent polar path for the interval− 1100 to− 670 my for North America. *Journal of Geophysical Research: Solid Earth*, *83*(B3), pp.1289-1304.

Swanson-Hysell, N.L., Vaughan, A.A., Mustain, M.R. and Asp, K.E., 2014a. Confirmation of progressive plate motion during the Midcontinent Rift's early magmatic stage from the Osler Volcanic Group, Ontario, Canada. *Geochemistry, Geophysics, Geosystems*, *15*(5), pp.2039-2047.

Swanson-Hysell, N.L., Burgess, S.D., Maloof, A.C. and Bowring, S.A., 2014b. Magmatic activity and plate motion during the latent stage of Midcontinent Rift development. *Geology*, *42*(6), pp.475-478.

Symons, D.T.A., Kawasaki, K. and Diehl, J.F., 2013. Age and genesis of the White Pine stratiform copper mineralization, northern Michigan, USA, from paleomagnetism. *Geofluids*, *13*(2), pp.112-126.

Tanaka, H. and Idnurm, M., 1994. Palaeomagnetism of Proterozoic mafic intrusions and host rocks of the Mount Isa Inlier, Australia: revisited. *Precambrian Research*, *69*(1-4), pp.241-258, doi: 10.1016/0301-9268(94)90089-2

Tauxe, L. and Kodama, K.P., 2009. Paleosecular variation models for ancient times: Clues from Keweenawan lava flows. *Physics of the Earth and Planetary Interiors*, *177*(1), pp.31-45.

Warnock, A.C., Kodama, K.P. and Zeitler, P.K., 2000. Using thermochronometry and low□temperature demagnetization to accurately date Precambrian paleomagnetic poles. *Journal of Geophysical Research: Solid Earth*, *105*(B8), pp.19435-19453.

Wingate, M.T., Pisarevsky, S.A. and Evans, D.A., 2002. Rodinia connections between Australia and Laurentia: no SWEAT, no AUSWUS?.*Terra Nova*, *14*(2), pp.121-128.

DR5: Interpreted affinity of crustal terranes in East Antarctica and geological evidence for 1.07—0.90 Ga plate boundary

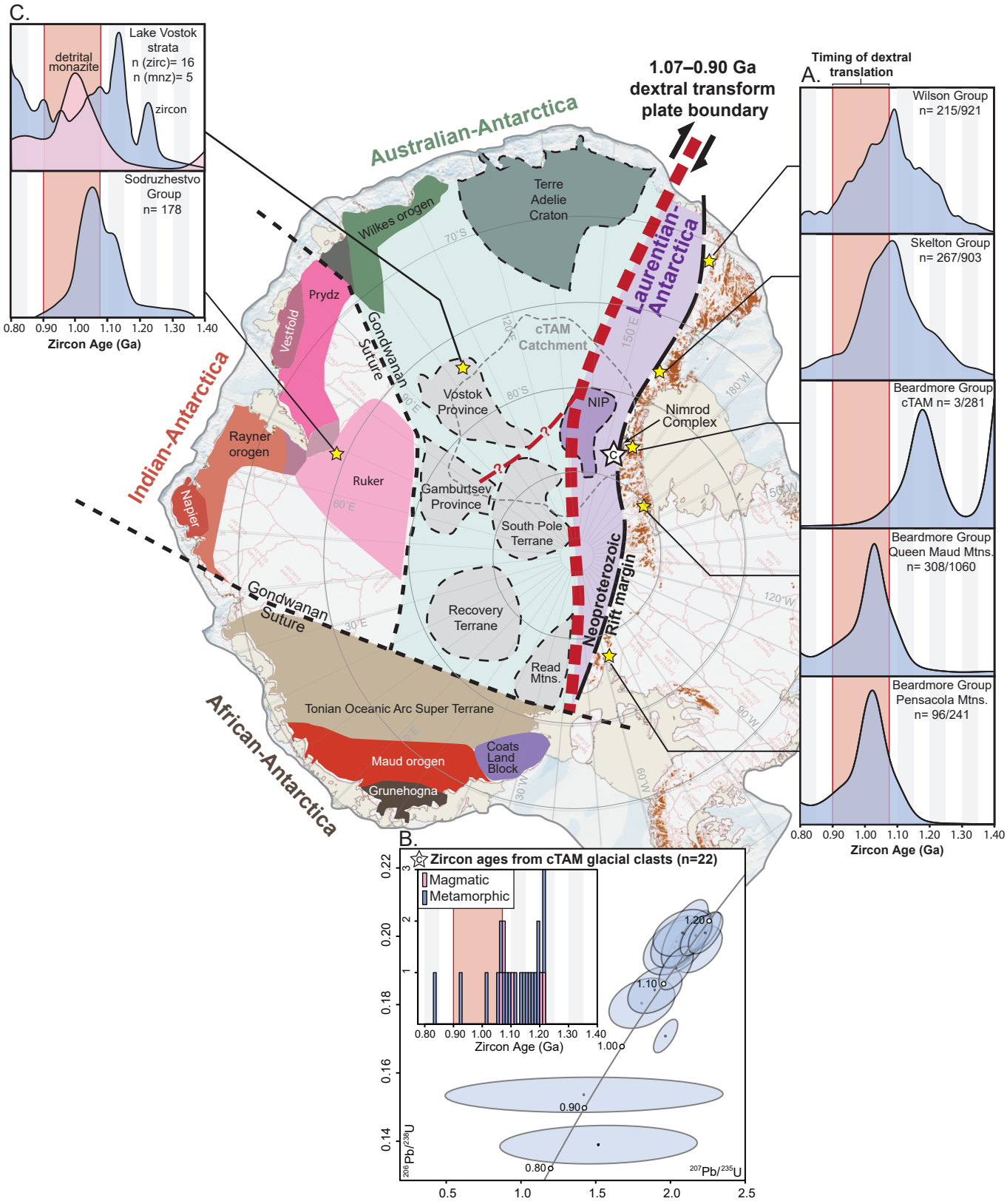

Figure DR5: Interpreted affinity of crustal terranes in East Antarctica and geological evidence for 1.07—0.90 Ga plate boundary

Affinity of terranes in East Antarctica are color-coded as follows: Australian (green shades) modified from Fitzsimons (2003), Goodge and Finn (2010), Aitken et al. (2014), Fanning and Goodge (2015), and Daczko et al. (2018); Indian (pink and red shades) from Flowerdew et al. (2013) and Aitken et al. (2014); African (brown shades) from Jacobs et al. (2015). The distribution of Laurentian crust (purple shades) is from this study with the extent of the Nimrod Igneous Province (NIP) and Coats Land Block from Goodge and Finn (2010) and Loewy et al. (2011), respectively. See accompanying references for detailed discussions supporting the affinity of the East Antarctic terranes. Ice-covered geophysically defined regions of inferred Archean/Paleoproterozoic crust of uncertain affinity are shown in grey with dashed outlines after Ferraccioli et al. (2011). We place these terranes within Australo-Antarctica to produce an approximately linear plate boundary between Australian and Laurentian crust, which facilitates simple dextral plate motion at 1.07—0.90 Ga (see also Figure 3B and C). The thin dashed red line shows an alternative extension of the 1.07—0.90 Ga plate boundary into a possible late Mesoproterozoic orogen within the Gamburtsev Province (Ferraccioli et al., 2011). Note that crust of Indian and African affinity was incorporated into East Antarctica during the Latest Neoproterozoic—early Paleozoic assembly of Gondwana (e.g., Fitzsimmons, 2003; Boger, 2011; Harley et al., 2013) and is not shown in the Figure 3 reconstructions of Rodinia. Base map source: https://www.add.scar.org/.

Geological evidence for the 1.07—0.90 Ga plate boundary includes: (Panel A) Abundant 1.07—0.90 Ga detrital zircons in Neoproterozoic strata in the Transantarctic Mountains, n= number of 1.07—0.90 Ga ages out of total concordant age population. (Panel B) Metamorphic zircon rims and Pb-loss trends from glacial clasts in the central Transantarctic Mountains (white star labelled 'C'). (Panel C) Common 1.07—0.90 Ga detrital zircon from the Neoproterozoic Sodruzhestvo Group in the Lambert Glacier, and detrital zircon and monazite from undated sedimentary rocks at Lake Vostok. References for zircon data are compiled in Table DR5-1.

Table DR5-1: Sources of zircon age data[1]

Unit	Location	Reference
Wilson Group	Northern Victoria Land	Paulsen et al. (2016), Estrada et al. (2016)
Skelton Group	Southern Victoria Land	Goodge et al. (2004), Paulsen et al. 2017
Beardmore Group	Central Transantarctic Mountains	Goodge et al. (2004), Goodge et al. (2002), Paulsen et al. (2017)
Beardmore Group	Queen Maud Mountains	Paulsen et al. (2017)
Beardmore Group	Pensacola Mountains	Goodge et al. (2004), Paulsen et al. (2017)
Glacial Clasts	central Transantarctic Mountains	Goodge et al. (2010), Goodge et al. (2017)
Sodruzhestvo Group	Lambert Glacier	Phillips et al. (2006)
Unnamed Sedimentary Rocks	Lake Vostok	Leitchenkov et al. (2011)

[1]Age calculations and discordance filters for zircon data follow Spencer et al. (2016).

REFERENCES

Aitken, A.R.A., Young, D.A., Ferraccioli, F., Betts, P.G., Greenbaum, J.S., Richter, T.G., Roberts, J.L., Blankenship, D.D., and Siegert, M.J., 2014, The subglacial geology of Wilkes Land, East Antarctica. Geophysical Research Letters v. 41, p. 2390–2400

Boger, S.D., 2011. Antarctica — Before and after Gondwana. Gondwana Research v. 19 (2), p. 335–371.
Harley, S.L., Fitzsimons, I.C.W., Zhao, Y., 2013. Antarctica and supercontinent evolution: historical perspectives, recent advances and unresolved issues. In: Harley, S.L., Fitzsimons, I.C.W. and Zhao, Y. (Eds.), Antarctica and Supercontinent Evolution, Geological Society, London, Special Publications v. 383, p. 1–34

Daczko, N. R., Halpin, J. A., Fitzsimons, I. C. W., and Wittaker, J. M., 2018, A cryptic Gondwana-forming orogen located in Antarctica. Scientific Reports v. 8:8371

Estrada, S., Läufer, A., Eckelmann, K., Hofmann, M., Gärtner, A., and Linnemann, U., 2016, Continuous Neoproterozoic to Ordovician sedimentation at the East Gondwana margin — Implications from detrital zircons of the Ross Orogen in northern Victoria Land, Antarctica. Gondwana Research v. 37, p. 426–448

Fanning, C. M., and Goodge, J. W., 2015, Role of the Nimrod Group, Central Transantarctic Mountains, in the Mawson Continent. XII International Symposium on Antarctic Earth Sciences Abstracts. p. 21–22

Ferraccioli, F., Finn, C.A., Jordan, T.A., Bell, R.E., Anderson, L.M., and Damaske, D., 2011, East Antarctic rifting triggers uplift of the Gamburtsev Mountains. Nature v. 479, p.388–392

Fitzsimons, I.C.W., 2003. Proterozoic basement provinces of southern and southwestern Australia, and their correlation with Antarctica. In: Yoshida, M., Windley, B.F., and Dasgupta, S. (Eds.), Proterozoic East Gondwana; supercontinent assembly and breakup: London, Geological Society of London Special Publications v. 206, p. 93–130

Flowerdew, M. J., Tyrrell, S., Boger, S. D., Fitzsimons, I. C. W., Harley, S. L., Mikhalsky, E. V., and Vaughn, A. P. M., 2013, Pb isotopic domains from the Indian Ocean sector of Antarctica: implications for past Antarctica-India connections. In: Harley, S. L., Fitzsimons, I. C. W. and Zhao, Y. (Eds.) 2013. Antarctica and Supercontinent Evolution. Geological Society, London, Special Publications v. 383, p. 59–72

Goodge, J.W., Myrow, P., Williams, I.S., and Bowring, S., 2002, Age and provenance of the Beardmore Group, Antarctica: constraints on Rodinia supercontinent breakup. Journal of Geology v. 110, p. 393–406

Goodge, J.W., Williams, I.S., Myrow, P., 2004. Provenance of Neoproterozoic and lower Paleozoic siliciclastic rocks of the central Ross Orogen, Antarctica: Detrital record of rift-, passive- and active-margin sedimentation. Geological Society of America Bulletin v. 116, p. 1253–1279

Goodge, J.W., Fanning, C.M., Brecke, D.M., Licht, K.J., and Palmer, E.F., 2010, Continuation of the Laurentian Grenville province in western East Antarctica. Journal of Geology v. 118, p. 601–619

Goodge, J.W., Fanning, M. C., Fisher, C. M., and Vervoort, J. D., 2017, Proterozoic crustal evolution of central East Antarctica: Age and isotopic evidence from glacial igneous clasts, and links with Australia and Laurentia. Precambrian Research v. 299, p. 151–176

Harley, S.L., Fitzsimons, I.C.W., and Zhao, Y., 2013, Antarctica and supercontinent evolution: historical perspectives, recent advances and unresolved issues. In: Harley, S.L., Fitzsimons, I.C.W. and Zhao, Y. (Eds.), Antarctica and Supercontinent Evolution. Geological Society London Special Publications v. 383, p. 1–34.

Jacobs, J., Elburg, M., Läufer, A.L., Kleinhanns, I.C., Henjes-Kunst, F., Estrada, S., Ruppel, A.S., Damaske, D., Montero, P., and Bea, F., 2015, Two distinct Late Mesoproterozoic/Early Neoproterozoic basement provinces in central/eastern Dronning Maud Land, East Antarctica: the missing link, 15–21°E. Precambrian Research v. 265, p. 249–272

Leitchenkov, G.L., Belyatsky, B.V., Rodionov, N.V., and Sergeev, S.A., 2007, Insight into the geology of the East Antarctic hinterland: a study of mineral inclusions from ice cores of the Lake Vostok borehole. In: Cooper, A.K., Raymond, C.R. (Eds.), Online Proceedings of the 10th ISAES, USGS Openfile Report 2007–1047, Short Research Paper 014

Loewy, S.L., Dalziel, I.W.D., Pisarevsky, S.A., Connelly, J.N., Tait, J., Hanson, R.E., and Bullen, D., 2011. Coats Land crustal block, East Antarctica: a tectonic tracer for Laurentia? Geology v. 39, p. 859–862

Paulsen, T. S., Deering, C., Sliwinski, J., Bachmann, O. and Guillong, M, 2016, Detrital zircon ages from the Ross Supergroup, north Victoria Land, Antarctica: Implications for the tectonostratigraphic evolution of the Pacific-Gondwana margin. Gondwana Research v. 35, p. 79–96

Paulsen, T. S., Deering, C., Sliwinski, J., Bachmann, O. and Guillong, M., 2017, Evidence for a spike in mantle carbon outgassing during the Ediacaran period. Nature Geoscience v. 10, p. 930—934

Phillips, G., Wilson, C.J.L., Campbell, I.H., and Allen, C.M., 2006. U–Th–Pb detrital zircon geochronology from the southern Prince Charles Mountains, East Antarctica—defining the Archaean to Neoproterozoic Ruker Province. Precambrian Research v. 148, p. 292–306

Spencer, C. J., Kirkland, C. L., and Taylor, R. J. M., 2016. Strategies towards statistically robust interpretations of in situ U-Pb zircon geochronology. Geoscience Frontiers v. 7, p. 581–589